Grasping Unknown Objects by Exploiting Shape Adaptability and Environmental Constraints

Clemens Eppner[1] and Oliver Brock[1]

Abstract— **In grasping, shape adaptation between hand and object has a major influence on grasp success. In this paper, we present an approach to grasping unknown objects that explicitly considers the effect of shape adaptability to simplify perception. Shape adaptation also occurs between the hand and the environment, for example, when fingers slide across the surface of the table to pick up a small object. Our approach to grasping also considers environmental shape adaptability to select grasps with high probability of success. We validate the proposed shape-adaptability-aware grasping approach in 880 real-world grasping trials with 30 objects. Our experiments show that the explicit consideration of shape adaptability of the hand leads to robust grasping of unknown objects. Simple perception suffices to achieve this robust grasping behavior.**

I. Introduction

In robots as well as in humans, grasp success is greatly affected by the ability of the hand to adapt to the shape of the object and the environment in response to contact forces. This adaptation increases the contact area and thereby the robustness of the grasp. Adaptation to the environment can either facilitate the attainment of robust grasp contacts through force interactions (e.g. sliding across the surface of a table to pick up a small object) or by avoiding premature contact that could prevent the attainment of robust grasp contacts.

The positive effect of shape adaptation on grasp success motivates the design of compliant, under-actuated gripper devices: The tendon-driven SDM hand [1] mechanically balances contact forces among its four flexible fingers. A gripper based on the jamming of granular material [2] can conform to a wide variety of object shapes. Deimel and Brock [3] developed a soft pneumatic hand that adapts to the object's shape through inflation. All of these examples show robust grasp performance through shape adaptation implemented in hardware, without explicit control or planning. In this paper, we exploit shape adaptation to simplify perception for grasping of unknown objects.

In human grasping, preshaping of the hand before contact occurs in a low-dimensional subspace of all possible hand configurations [4]. This provides further motivation for our grasping approach. It implies that large variability in grasp posture can be obtained from simple actuation. Indeed, this concept has also been implemented in robotic hands [5]. Our grasp approach uses simple controllers to generate finger motion and "lets the fingers fall where they may" [6] (shape adaptation) to achieve robust grasping.

Deliberate shape match between the hand and the environment can also increase grasp success. Humans, particularly when grasping small objects from flat surfaces, place their fingertips not directly on the object but slide them along the surrounding surface towards it. This observation motivates compliant, multi-stage control schemes to re-create this behavior [7].

Finally, shape match between object and environment can further improve grasp success. It occurs, for example, when objects adjust their position relative to the hand during grasping. In the context of bin-picking, simple grippers can take advantage of this kind of object compliance to achieve robust grasping [6]. The push-grasping approach also relies on such interactions between hand, object, and environment to improve grasping in the presence of sensing uncertainty and clutter [8]. Other approaches introduce pre-grasp manipulation actions to change the configuration of an object so as to facilitate grasping [9].

In this paper, we present shape-adaptation-aware grasping strategies for unknown objects. These strategies exploit hand/object and hand/environment shape adaptation in two ways. First, hand/object shape adaptation allows us to simplify perception. The shape adaptability of the hand adjusts to variations in object shape. Consequently, perception only needs to determine object shape to the level of detail not compensated by shape adaptation. The loss in geometric accuracy of the acquired object model is compensated by the shape adaptability of the hand. Second, hand/environment shape adaptation further increases grasp success. Instead of viewing the environment as an obstacle with which contact is to be avoided, our approach optimizes the grasping strategy based on the constraints induced by the environment.

We present experimental evidence in support of the proposed shape-adaptation-aware grasp approach. We validate the suitability of our perceptual primitives to exploit shape adaptability in 420 real-world grasping trials with 21 objects. We further demonstrate the beneficial effect of considering hand/environment shape match in 460 real-world grasping trials with 23 objects. Our results show that the consideration of shape adaptability in grasping leads to robust, effective, and simple grasping strategies in the absence of a priori object models.

II. Related Work

We examine the use of hand-object and hand-environment shape adaptation in the grasping literature, emphasizing

We gratefully acknowledge the funding provided by the Alexander von Humboldt foundation and the Federal Ministry of Education and Research (BMBF) and through the First-MM project (European Commission, FP7-ICT-248258). We thank SimLab for their support.

[1]Robotics and Biology Laboratory, Technische Universität Berlin, Germany

methods that do not require a priori object knowledge.

By far the most common use of hand-object shape adaptation is the approximation of object models by a limited set of primitives. Each primitive is associated with a grasping action. Huebner and Kragic [10] use boxes to approximate shapes, Przybylski et al. [11] propose inscribing balls, and [12] decompose shapes into superquadrics. All of these approaches require complete object models. The problem of perception, which is the focus of this paper, is ignored.

Another group of methods uses the same approach to shape adaptation but partially addresses the perception problem. Papazov et al. [13] recognizes known objects in a scene based on sensor data and uses the associated exact model to plan grasps. In a similar fashion, [14] recognizes objects in the scene based on a decomposition of given CAD models. The perception of these methods still requires complete a priori object models.

The next category of related approaches exploits aspects of shape adaptability between hand and object and also addresses the perception problem. However, each of these methods has limitations overcome by our approach. In our discussion, we do not consider collision avoidance during grasping as an appropriate consideration of hand/environment shape adaptation.

In one of the earliest approaches that exploit shape matching, the authors map bounding ellipses extracted from an image to three different hand preshapes of two-fingered hand [15]. This method is restricted to "grasping from the top" and does not consider environmental constraints. Kootstra et al. [16] extract contour and surface features from visual input. The features are mapped to grasping actions: enveloping grasps for surfaces and pinch grasps for contours. This method does not consider interactions with the environment. A method proposed by Klingbeil et al. [17] searches for protrusions in range scans as candidate locations for grasping with a parallel-yaw gripper, but not with multi-fingered hands. Herzog et al. [18] learns graspable 3-D features in the environment from human demonstration. They side-step the perception problem with human input. [19] propose an approach that learns hand-object shape matches: two classifiers are trained to select promising grasps based on 2-D image features and 3-D volumetric features. They do not consider interactions with the environment. Maldonado et al. [20] assume that all objects are placed on top of a table. Each point cluster above the table surface is interpreted as an object. The pre-grasp pose is optimized to bring the center of the palm as close to the object while maximizing the distance between object and fingers.

III. Representing shape adaptability in grasping

We consider the problem of power grasping with multi-fingered hands in the absence of a priori object models. We focus on aspects of object capture and grasp stability under variations of object shape for a given robotic hand. We show that shape-adaptation-aware grasping leads to robust grasping performance and significantly reduces the requirements on perception.

Fig. 1: The motion of two different preshapes of the Barrett Hand. To find suitable grasps we search for structure that is shaped complementarily.

The general underlying idea of our method is to characterize the match between the shape of an arbitrary unknown object and the complimentary shape of a known hand that it traverses during a grasping motion. We observed in grasping experiments that the final success is significantly influenced by the match of the hand with the environment. Later, we will therefore also introduce a simple model that predicts and exploits this effect.

A. Shape match between hand and object

Our method uses the popular Barrett Hand as an example for a multi-fingered hand. We abstract the hand geometry into a set of preshapes – configurations that define the internal degrees of freedom of the hand. This is a common concept, e.g. see [21]. In the case of the Barrett Hand we identify two preshapes: a spherical and cylindrical (see Fig. 1). The idea is that the closing motion of these preshapes match a large variety of possibly occurring object shapes.

We introduce four different shape descriptors: a spherical, cylindrical, box, and disk one. Each one is supposed to recognize a different subset of all possible object shapes. They exploit the shape adaptability of the hand: Starting from a preshape a closing motion is executed which only stops at motor stall. The Barrett Hand also possesses a break-away mechanism: Each finger is actuated by a single motor which distributes its torque to two finger joints. Once the proximal link's motion is inhibited by an external contact force, the motor torque is solely applied to the distal link. This mechanical mechanism adds shape adaptability, thus demanding less restrictive shape descriptors. We now explain how the four descriptors work, based on depth image measurements taken by any time-of-flight, stereo or structured-light sensor.

We avoid the highly non-convex parameter space that occurs when fitting geometric models to raw sensor data by first segmenting it. As there is no single-best segmentation for the different shapes we are looking for we apply multiple ones. A flood fill algorithm similar to [22] segments the depth image into coherent regions. This segmentation groups neighboring points o and p according to a boolean predicate, which we define as follows:

$$\begin{aligned} |o_{\text{depth}} - p_{\text{depth}}| &< t_{\text{depth}} \quad \wedge \\ \langle o_{\vec{\text{normal}}}, p_{\vec{\text{normal}}} \rangle &< t_{\text{angle}} \quad \wedge \\ o_{\text{curvature}} &< t_{\text{curvature}}, \end{aligned}$$

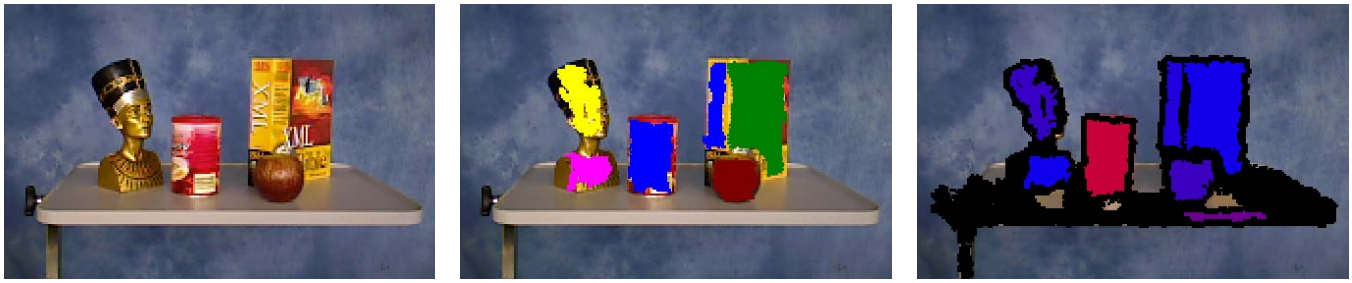

Fig. 2: To improve clarity the depth values are plotted on top of the camera image, although our method only uses range data. The center image shows the result of one flood fill segmentation that separates the geometry at depth discontinuities and sharp edges. The segments are then described by different shape descriptors to match the hand geometry. The right image depicts the cylindrical shape descriptor ranging from red (very cylindrical) to blue (hardly cylindrical).

where o_{depth} is the depth of point o, $o_{\vec{\text{normal}}}$ its surface normal, $o_{\text{curvature}}$ its mean curvature, and $(t_{\text{depth}}, t_{\text{angle}}, t_{\text{curvature}})$ a set of thresholds. Small-sized segments are filtered out. We use segmentations with low $t_{\text{curvature}}$ and t_{angle} which favor edge boundaries and high values of t_{depth} that result in larger regions even in the presence of noise. The resulting segment soup builds the basis for our different shape descriptors. They all fit geometric models to the segments using the method of Random Sample Consensus (RANSAC). A large threshold in the inlier criterion allows for considerable shape variation which we assume can be compensated by the hand's closing motion. The goodness of fit is described differently for each geometry:

Spherical Shape Descriptor: A sphere is fit with a radius bounded to the range graspable by the Barrett Hand's spherical preshape. The goodness of fit is based on the ratio of inliers and segment size in combination with the visibility of the hypothesized sphere. The visibility criterion is the ratio of the segment size and the expected size of the sphere backprojected into the sensor frame.

Cylindrical Shape Descriptor: An infinitely tall cylinder is fitted which is bounded by the extreme inliers along the cylinder's axis. The height and radius are again constrained by the hand geometry. A goodness of fit value is given by the ratio of inliers and segment size in combination with the expected visibility analog to the spherical shape descriptor.

Box Shape Descriptor: A plane fit is bounded by projecting its inliers orthogonal onto the plane and calculating the 2D minimum enclosing rectangle. If the rectangle size exceeds the graspable volume of the cylindrical preshape it is discarded. The goodness of fit is a combination of the inlier ratio and the rectangularity of the contour of the projected points. This rectangularity is defined as the ratio of the area of the convex hull and the fitted rectangle.

Disk Shape Descriptor: The disk descriptor works similar to the box descriptor with the exception that it uses the minimum enclosing circle of the projected points to define the goodness of fit instead of a rectangle.

Fig. 2 shows an example application of the cylindrical shape descriptor.

B. From single pre-grasps to pre-grasp regions

The previously defined shape descriptors not only imply a preshape and closing motion of the hand but also its pose in 3d space. This is straightforward given the geometric models: The cylinder gives rise to two pre-grasps, both parallel to the cylinder's axis with the thumb pointing left or right. The box descriptors results in four possible poses, two along each pair of parallel edges. Disk and spherical descriptors create pre-grasps whose approach vector points towards their centers.

Instead of single poses we define whole regions by exploiting the symmetry of the shape descriptors. A pre-grasp region is defined by a curvilinear coordinate system depending on the grasp's preshape. In the cylindrical case the pre-grasp region is given by cylindrical coordinates with a fixed radius. The analogs for all other strategies are depicted in Fig. 3. Going from single pre-grasp poses to whole regions allows us to satisfy environmental constraints as we will show next.

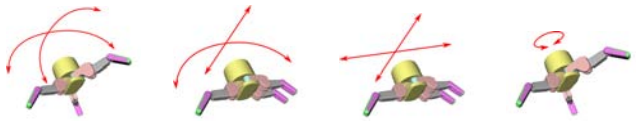

(a) Spherical (b) Cylindrical (c) Box (d) Disk

Fig. 3: The four different preshapes and their associated curvilinear coordinates (red arrows) that make up the pre-grasp regions. Cylindrical and spherical regions are represented by cylindrical and spherical coordinates; the box region exhibits one translational degree of freedom while the disk region is defined about one axis of rotation. These regions are used to further refine the pose of a pre-grasp.

C. Shape match between hand and environment

Think about a bottle laying flat on a table. Even if you see it from the front, your palm will most likely approach it from above parallel to the table surface, with the fingers touching the table while the fingers bend around the object. Instead of avoiding the table it is exploited. A controller that imitates this behavior successfully was shown in [7].

We anticipate this shape match between the hand's closing motion and its immediate environment by refining the pre-

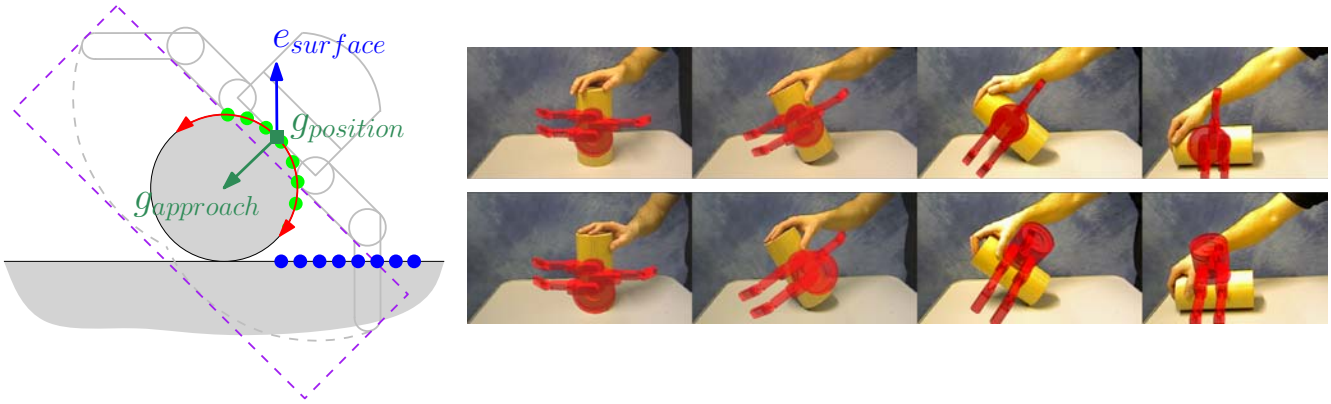

(a) (b)

Fig. 4: In **(a)** a 2d explanation of the environmental adaptation scheme is shown. Assume we have given range sensor readings (bold dots), a segmentation (dot's colors), a pre-grasp (grey two-fingered hand model with approach vector g_{approach} and position g_{position}) and its associated 1d region (red half circle). The mean surface normal e_{surface} of the environment is the average over all measured surface normals that fall within the expected closing region (purple rectangle) and are not part of the segment to be grasped. We choose the pre-grasp from the region that minimizes a cost which includes the difference between $-g_{\text{approach}}$ and e_{surface} and the distance of g_{position} to the region's origin. See text for details. **(b)**: *Upper row:* Shape match with the environment is ignored. The cylinder is always grasped from the front. *Lower row:* The closer the cylinder is to the table surface the more the pre-grasp pose tries to match with it.

grasp pose within its respective pre-grasp region. The environmental constraints are extracted by analyzing the depth measurements that fall within the closing volume of the hand: The number of points intersecting this volume g_{points}, the maximum possible number $g_{\text{maxpoints}}$, and their mean surface normal e_{surface} are computed. We refine the pre-grasp pose by casting it as an bounded optimization problem. The objective function is given as the weighted sum of the orientation error (between grasp approach and surface normal) and the distance to the origin of the pre-grasp region:

$$\underset{(g_{\text{position}},g_{\text{approach}})}{\text{argmin}} \left(w \frac{g_{\text{points}}}{g_{\text{maxpoints}}} \langle -g_{\text{approach}}, e_{\text{surface}} \rangle + d(g_{\text{position}}, 0) \right),$$

where $d(\cdot,\cdot)$ is a distance measure depending on the curvilinear coordinates used, and w is a weight which balances the amount of shape match with the environment versus preferring known zones inside the pre-grasp region. A graphical explanation is depicted in Fig. 4 along with an example for a cylindrical pre-grasp optimization on real sensor data. We have implemented and applied this optimization for the cylindrical and spherical pre-grasp strategy.

To model the accessibility of a pre-grasp pose we add an additional term which depends on the free space along the approach vector. Therefore we sweep the hand volume through the depth image and count the colliding points. Apart from penalizing hard to reach grasps, it also rejects false positives due to concave shapes.

Finally, we track grasp hypotheses over time by associating the most similar ones in successive time steps. Similarity is based on pre-grasp configuration and pose. During tracking we filter out hypothesis that do not appear with a frequency of at least $\sim$ 3 Hz. This eliminates unstable hypotheses caused by sensor noise.

All pre-grasp descriptors run in parallel and do not influence each other. Because we are not interested in subtle geometric features we can rely on a rather coarse depth image resolution of 320 $\times$ 240. This additionally speeds up our processing pipeline, resulting in $\sim$ 5.3 Hz on a standard desktop computer at 2.2GHz using a single-threaded implementation. Roughly 70% of the load are produced by fitting the primitives and normal estimation.

IV. Experimental Evaluation

The goal of our experiments is to examine how well our perceptual grasping strategies can predict their success: First based on the match between object and hand, then including a simple environmental constraint in form of a table surface, and finally in an exemplary cluttered scene, where environmental constrains are more complex due to multiple objects.

V. Experimental Setup

A Unimation PUMA 560 with 6-DoF was equipped with a Barrett Hand BH8-262 and an Asus Xtion Live depth sensor based on structured light. The sensor was mounted on the wrist as can be seen in Fig. 1. During each grasping trial the robot was observing an object for 3 seconds from a single view point. During that time it chose the most promising pre-grasp strategy. If no pre-grasp confidence exceeded a predefined threshold, no grasp was executed and the next view point was considered. Otherwise, a force-based operational space control law was executed to approach the planned pre-grasp pose from an intermediate pose located 10 cm in the negative direction of the approach vector. During the final stage of the motion the operational space gains were lowered in all dimensions to make the arm more compliant. After reaching the pre-grasp pose, the hand was preshaped and a closing motion executed. We counted a grasp to be successful

Fig. 5: The test objects used throughout the experiments.

if it could lift the object 30 cm and pertained to the hand for 10 seconds.

A. Shape Match between Hand and Object

To measure the predictability of hand/object match of our pre-grasp strategies, we conducted a simplified experiment that excluded any environmental constraints. 21 objects 5 were placed onto a sticky tripod. This resembled a quasi-static scenario free of any effects induced by interactions between hand and environment. Each object was placed 5 times in different orientations in front of the robot. For each strategy we measured the rate of pre-grasp detection and grasp success as defined above. The results shown in Fig. 6 largely confirm our intuition: Whenever a promising grasp was predicted by one of the descriptors, the likelihood that the corresponding grasp also succeeded was high. Note, that although there are partial overlaps between strategies no strategy is dominated by another one and thereby obsolete. Finally, all of the analyzed objects were grasped by at least one of the strategies, showing that together they cover a significant amount of possible occuring object shapes.

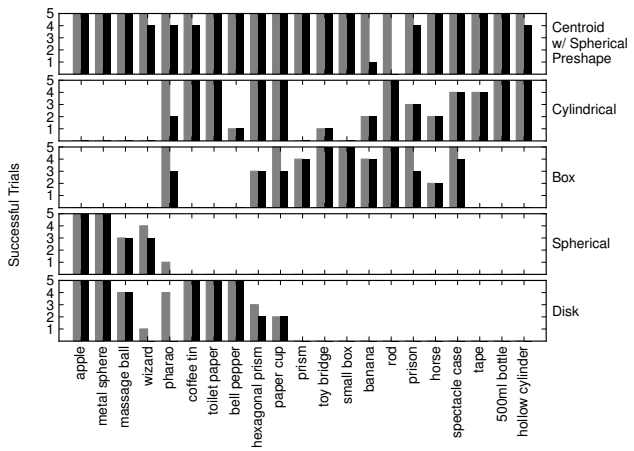

Fig. 6: Grasping performance in the no-environmental-constraint condition for each of the four pre-grasp strategies and a strategy which approached the objects towards the perceived centroid from the current view point with a spherical preshaped hand. The light-colored bar indicates a predicted grasp by the algorithm. The dark-colored one is the resulting grasp success.

Fig. 7: The experimental setup for the simple environmental contraints: The sensor observes the object from the five different perspectives shown.

Additionally, we executed a comparative strategy that approached the object's centroid along the ray originating from the camera's view point. The results shown in the first row of Fig. 6 indicate that this simple strategy already exploits enough information to grasp successfully.

B. Shape Match under simple environmental constraints

Apart from the hand/object match we continued analyzing the impact of environmental constraints by placing objects onto a table. 23 different objects were observed from five different viewpoints as shown in Fig. 7. For each object the four strategies were again evaluated independently, resulting in a total of 460 trials. The resulting detection and success rates are depicted in 8. The overall grasping performance decreases with respect to the prior condition as could be expected due to the more realistic setting. Still, success can be predicted most of the time reliably with a few exceptions: The globe and wizard are close to prototypical spheres, but they exhibit low frictional surfaces which in combination with the aluminum cover of the Barrett Hand require very high contact forces to be grasped successfully. Another problem – especially with the spherical preshapes – was a pre-mature activation of the breakaway mechanism. Fingers stopped even when not in contact with object. Note though, that again only few objects cannot be detected by any of the proposed strategies: One such case is the flat laying tape which exhibits a disk-shaped top face which was not detected because of the low resolution of the sensor and the minimum distance it needs to maintain during sensing.

Some example grasps can be seen in Fig. 9. They show that the proposed strategies can successfully exploit shape match with the environment.

C. Shape Match under complex environmental constraints

In a final experiment, we wanted to test how well our methods scales with more complex scenes, in which multiple objects can also constrain each other. The promising result of

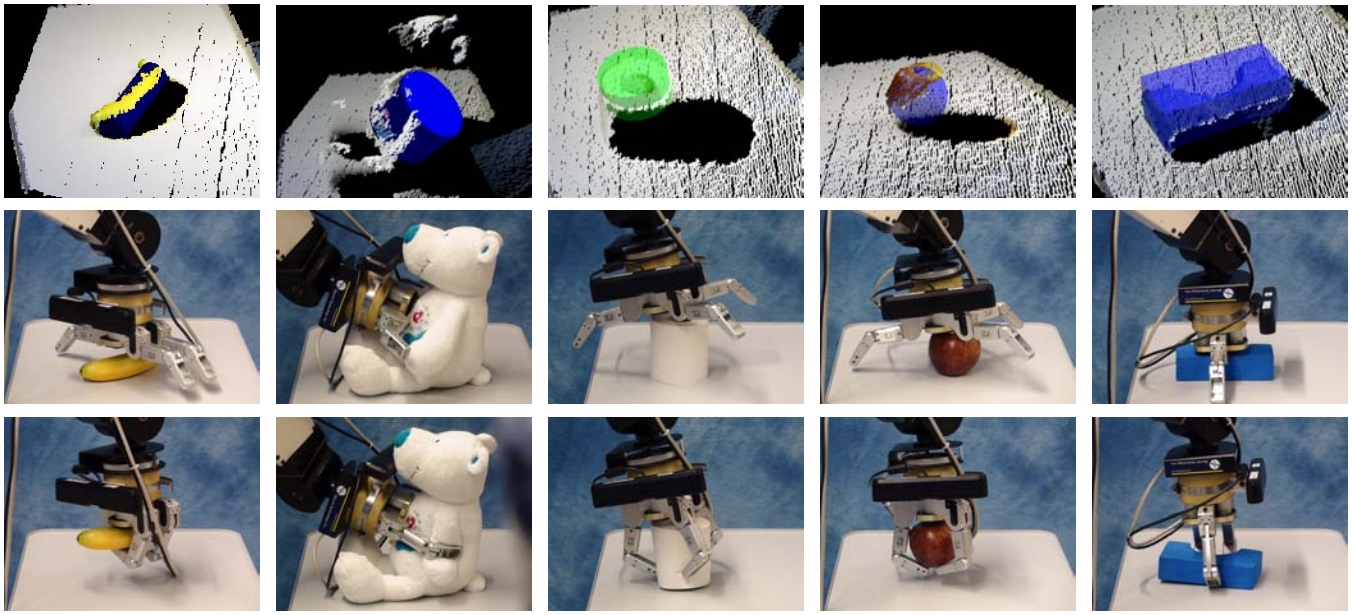

Fig. 9: Some exemplary grasps from the experiments with environmentally constrained objects: The first row shows the fitted geometric models (from left to right: two cylinders, disk, sphere, box) within the pointcloud perceived by the robot. The second and third row show the resulting pre-grasps and final grasps executed by the robot.

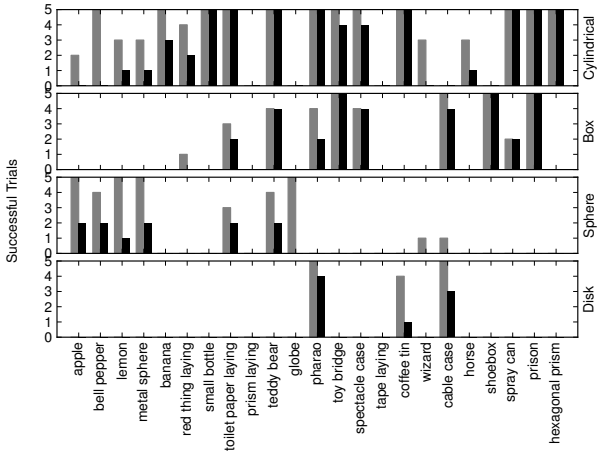

Fig. 8: Grasping performance in the environmental-constraint condition for each of the four pre-grasp strategies. The light-colored bar indicates a predicted grasp by the algorithm. The dark-colored one is the resulting grasp success.

Fig. 10: A small cluttered scene used in the last experiment.

an example with five objects is shown in Fig. 11. The robot observed the scene five times from the same view point, each time selecting the most promising grasp. Note, that our method has no notion of gravity or whether two grasps belong to the same object. Still, the accessibility criterion implicitly favors most of the time shape matches that are on top of each other. In this qualitative experiment the robot only failed grasping the last object, a bottle which was located close to the edge of the table. Overall the results for the cluttered scene are pointing in a promising direction.

VI. Conclusion

We presented a shape-adaptation-aware approach to grasping of unknown objects. There is much evidence in the human and robot grasping literature that shape adaptation significantly increases grasping success. We therefore explicitly account for the effects of shape adaptation in the design of grasping algorithms. The proposed method considers shape adaptation between the hand and the grasped object to simplify perception. Rather than attempting to perceive the exact shape of the object to perform grasp planning, we assume that the shape must only be known to the level of detail necessary to decide which pre-grasp is most appropriate. The pre-grasp then invokes a particular mode of shape adaptation of the hand by closing the fingers, compensating for any infidelities in the perceived object model. Further, the proposed method accounts for shape matching between the hand and the environment by selecting

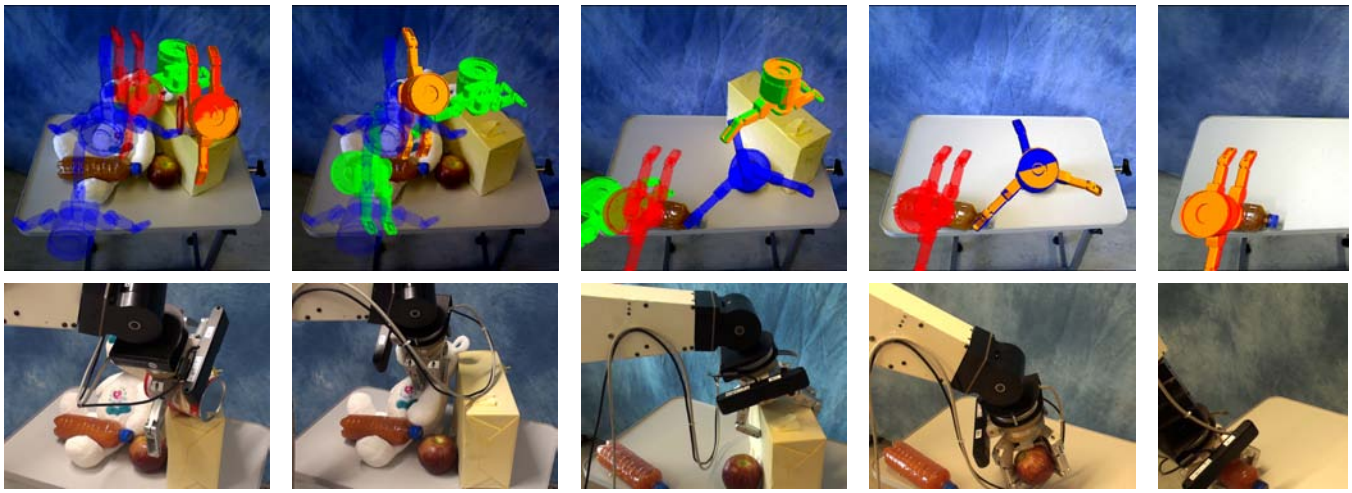

Fig. 11: The five different decisions to empty the table are shown from left to right. The upper row shows the view of the sensor with the possible pre-grasp poses (green = box, blue = sphere, red = cylinder). Each time the robot chose the most promising pre-grasp (displayed in golden color) based on shape match with the object and environment. The lower row shows the grasps executed by the robot. All except the last were successful.

a grasp from the set of all grasp postures that maximizes expected grasp success based on environmental constraints. Our experiments demonstrate that the explicit consideration of shape adaptability reduces the perceptual requirements of grasping and enables robust grasp performance without explicit planning of contact points.

REFERENCES

[1] A. M. Dollar and R. D. Howe, "The highly adaptive SDM hand: Design and performance evaluation," *The Intl. Journal of Robotics Research*, vol. 29, no. 5, pp. 585 –597, 2010.

[2] E. Brown, N. Rodenberg, J. Amend, A. Mozeika, E. Steltz, M. R. Zakin, H. Lipson, and H. M. Jaeger, "Universal robotic gripper based on the jamming of granular material," *Proceedings of the National Academy of Sciences*, vol. 107, no. 44, pp. 18 809–18 814, 2010.

[3] R. Deimel and O. Brock, "A compliant hand based on a novel pneumatic actuator," in *Proceedings of the IEEE International Conference on Robotics and Automation (ICRA)*, 2013.

[4] M. Santello, M. Flanders, and J. F. Soechting, "Postural hand synergies for tool use," *The Journal of Neuroscience*, vol. 18, no. 23, pp. 10 105 –10 115, 1998.

[5] C. Brown and H. Asada, "Inter-finger coordination and postural synergies in robot hands via mechanical implementation of principal components analysis," in *IEEE/RSJ International Conference on Intelligent Robots and Systems*, 2007, pp. 2877 –2882.

[6] M. T. Mason, A. Rodriguez, S. Srinivasa, and A. Vazquez, "Autonomous manipulation with a general-purpose simple hand," *The Intl. Journal of Robotics Research*, 2011.

[7] M. Kazemi, J. S. Valois, J. A. Bagnell, and N. Pollard, "Robust object grasping using force compliant motion primitives," Tech. Rep. CMU-RI-TR-12-04, 2012. [Online]. Available: http://www.ri.cmu.edu/pub_files/2012/1/CMU_RI_TR_compliant_grasp.pdf

[8] M. Dogar and S. Srinivasa, "Push-grasping with dexterous hands: Mechanics and a method," in *2010 IEEE/RSJ Intl. Conf. on Intelligent Robots and Systems (IROS)*, 2010, p. 21232130.

[9] D. Kappler, L. Chang, M. Przybylski, N. Pollard, T. Asfour, and R. Dillmann, "Representation of pre-grasp strategies for object manipulation," in *IEEE-RAS International Conference on Humanoid Robots*, 2010.

[10] K. Huebner and D. Kragic, "Selection of robot pre-grasps using box-based shape approximation," in *Intelligent Robots and Systems, 2008. IROS 2008. IEEE/RSJ Intl. Conf. on*, 2008, pp. 1765—1770.

[11] M. Przybylski, T. Asfour, and R. Dillmann, "Unions of balls for shape approximation in robot grasping," in *2010 IEEE/RSJ Intl. Conf. on Intelligent Robots and Systems (IROS)*, 2010, pp. 1592–1599.

[12] C. Goldfeder, P. K. Allen, C. Lackner, and R. Pelossof, "Grasp planning via decomposition trees," in *2007 IEEE Intl. Conf. on Robotics and Automation*, 2007, pp. 4679–4684.

[13] C. Papazov, S. Haddadin, S. Parusel, K. Krieger, and D. Burschka, "Rigid 3d geometry matching for grasping of known objects in cluttered scenes," *The International Journal of Robotics Research*, vol. 31, no. 4, pp. 538–553, 2012. [Online]. Available: http://ijr.sagepub.com/content/31/4/538.abstract

[14] M. Nieuwenhuisen, J. Stückler, A. Berner, R. Klein, and S. Behnke, "Shape-primitive based object recognition and grasping," *ROBOTIK 2012*, 2012. [Online]. Available: http://www.vde-verlag.de/proceedings-en/453418085.html

[15] C. Bard and J. Troccaz, "Automatic preshaping for a dextrous hand from a simple description of objects," in *Intelligent Robots and Systems' 90.'Towards a New Frontier of Applications', Proceedings. IROS'90. IEEE International Workshop on*, 1990, p. 865872. [Online]. Available: http://ieeexplore.ieee.org/xpls/abs_all.jsp?arnumber=262507

[16] G. Kootstra, M. Popovic, J. A. Jorgensen, K. Kuklinski, K. Miatliuk, D. Kragic, and N. Kruger, "Enabling grasping of unknown objects through a synergistic use of edge and surface information," *The International Journal of Robotics Research*, vol. 31, no. 10, pp. 1190–1213, Aug. 2012. [Online]. Available: http://ijr.sagepub.com/cgi/doi/10.1177/0278364912452621

[17] E. Klingbeil, D. Rao, B. Carpenter, V. Ganapathi, A. Y. Ng, and O. Khatib, "Grasping with application to an autonomous checkout robot," in *2011 IEEE Intl. Conf. on Robotics and Automation (ICRA)*, 2011.

[18] A. Herzog, P. Pastor, M. Kalakrishnan, L. Righetti, T. Asfour, and S. Schaal, "Template-based learning of grasp selection," in *Robotics and Automation (ICRA), 2012 IEEE International Conference on*, 2012, p. 23792384. [Online]. Available: http://ieeexplore.ieee.org/xpls/abs_all.jsp?arnumber=6225271

[19] A. Saxena, L. Wong, and A. Y. Ng, "Learning grasp strategies with partial shape information," in *Proceedings of the 23rd national conference on Artificial intelligence*, 2008, p. 14911494.

[20] A. Maldonado, U. Klank, and M. Beetz, "Robotic grasping of unmodeled objects using time-of-flight range data and finger torque information," in *2010 IEEE/RSJ International Conference on Intelligent Robots and Systems (IROS)*, Taipei, Taiwan, October 18-22 2010, pp. 2586–2591.

[21] A. Miller, S. Knoop, H. Christensen, and P. Allen, "Automatic grasp planning using shape primitives," in *Robotics and Automation, 2003. Proceedings. ICRA '03. IEEE Intl. Conf. on*, vol. 2, 2003, pp. 1824–1829 vol.2.

[22] D. Holz, J. B. Trevor, M. Dixon, S. Gedikli, and R. B. Rusu, "Fast segmentation of RGB-D images for semantic scene understanding," 2012. [Online]. Available: http://www.ais.uni-bonn.de/papers/ICRA_SPMK_2012_Holz.pdf